Technical Paper by R.S. Thiel

DESIGN METHODOLOGY FOR A GAS PRESSURE RELIEF LAYER BELOW A GEOMEMBRANE LANDFILL COVER TO IMPROVE SLOPE STABILITY

ABSTRACT: Pore pressures generated by landfill gas underneath a final cover system that incorporates a geomembrane can significantly reduce the effective normal stress on the lower geomembrane interface to the point of creating cover veneer instability. To the author's knowledge, no design methodology has previously been published to address this issue. Recently, however, large-scale slope failures have been attributed to landfill gas pore pressures. Therefore, a need for a design methodology exists. An estimation of gas flux from a landfill surface can allow a gas-relief layer to be designed using Darcy's law for gas flow through a porous medium. The methodology incorporates knowledge of the gas transmissivity of a chosen medium to design a spacing for highly permeable strip drains. The strip drains in turn can discharge the gas either to vents or an active gas collection system. The gas-relief layer typically consists of sand or a geonet composite. Limited testing of nonwoven, needle-punched (NWNP) geotextiles indicates that these materials may also be acceptable for gas relief in some designs. However, more testing is recommended before using NWNP geotextiles alone in this application. The greatest assumption in the proposed methodology concerns the estimation of gas flux. More research is required in this regard; however, the basic concept of providing a gas-relief layer with intermittent highly permeable strip drains is recommended as a prudent engineering measure for landfill final cover systems incorporating geomembrane barriers.

KEYWORDS: Geomembrane, Landfill cover, Slope stability, Landfill gas.

AUTHOR: R.S. Thiel, Principal, Thiel Engineering, P.O. Box 1010, Oregon House, California 95962, USA, Telephone: 1/530-692-9114, Telefax: 1/530-692-9115, E-mail: rickthiel@aol.com.

PUBLICATION: *Geosynthetics International* is published by the Industrial Fabrics Association International, 1801 County Road B West, Roseville, Minnesota 55113-4061, USA, Telephone: 1/651-222-2508, Telefax: 1/651-631-9334. *Geosynthetics International* is registered under ISSN 1072-6349.

DATES: Original manuscript received 21 August 1998, revised version received 22 October 1998 and accepted 20 November 1998. Discussion open until 1 July 1999.

REFERENCE: Thiel, R.S., 1998, "Design Methodology for a Gas Pressure Relief Layer Below a Landfill Geomembrane Cover to Improve Slope Stability", *Geosynthetics International*, Vol. 5, No. 6, pp. 589-617.

1 INTRODUCTION

Landfill gas is continuously generated in landfills as the waste decomposes. The concern for final landfill cover designs incorporating geomembranes is that an uplift pressure can be caused by the gas. From a slope stability point of view, gas pressure is an excess pore pressure that serves to reduce the effective normal stress. Classic soil mechanics methods provide all of the necessary tools to address the slope stability of landfill covers, including the effects of gas pressure. However, what has been lacking to date are: (i) an explicit recognition of gas pressures as a design issue for landfill covers; (ii) a methodology to incorporate the fluid mechanics calculations of gas (versus water) in the slope stability analyses; and (iii) an understanding of how to estimate gas-relief requirements. The current paper attempts to address points (i) and (ii) above, and provides guidelines and experience relative to point (iii). However, estimation of landfill gas generation rates, and the resulting flux from the upper surface, is beyond the expertise of the author and, in the author's experience, is more of an art than a science even for the gas "experts".

2 OUTLINE OF GAS PRESSURE RELIEF LAYER DESIGN

The following are the three primary steps for designing the gas pressure relief layer:

1. Estimate the maximum flux of gas below the landfill final cover that may need to be removed. The units of flux are volume per surface area per unit time, such as cubic meters of gas per hour per square meter of landfill surface ($m^3/hr/m^2$).
2. Perform slope stability analyses to estimate the maximum allowable gas pressure that results in an acceptable overall static factor of safety. In this case, the designer can use any cover slope stability model deemed appropriate for the project, but must be able to incorporate gas pore pressures from below the landfill cover, as described in Section 4.

   In the literature, there are several papers describing landfill cover veneer slope stability (Koerner and Soong 1998; Kavazanjian 1998; Thiel and Stewart 1993). In these papers, different considerations for cover slope stability are presented and developed, including infinite slope approaches, seepage forces, seismic forces, toe buttressing forces, tapered slopes, and slope reinforcement. It is left to the individual practitioner to select the model and develop the design most appropriate for a given situation. In the interests of brevity, the slope stability equations used in the current paper for the development of gas pressure considerations are limited to nonreinforced, static, infinite-slope conditions. However, the principles developed herein to include gas pressures in a stability analysis can easily be combined with other models as well.
3. Design a passive vent system below the cover that evacuates the gas at a flow rate that matches the design flux calculated in Step 1 above and under the maximum allowable driving pressure determined in Step 2.

Each of the three steps summarized above is described in detail in Sections 3, 4, and 5, respectively.

3 ESTIMATION OF GAS FLUX

The mass flux of gas from the surface of a landfill, Φ_g , is site specific and varies spatially and temporally in a given landfill. The amount of gas depends on the waste type, age, temperature, moisture, other avenues of gas extraction or venting, and barometric pressure. The literature reports landfill gas generation rates up to 0.037 standard cubic meters per wet kilogram of waste per year (0.037 m^3/kg/yr) (Pacey 1997). However, this value is exceptionally high and is reported for controlled landfills in an enhanced decomposition mode. For closures at municipal solid waste landfills in the northwestern United States, where cell closure occurs at the end of a cell's life, the author frequently uses a gas flux of 6.24×10^{-3} m^3/kg/yr for purposes of cover design. When using gas modeling computer programs, the author recommends that the upper section of the gas estimation curve be utilized for purposes of cover slope stability. Estimation of the flux rate is very site specific and is beyond the scope of the current paper.

Example 1. Gas Flux Calculation

Given an average waste depth of 30 m, a waste density, ϱ_{waste} , of 800 kg/m^3, and a landfill gas generation rate, r_g , of 6.24×10^{-3} m^3/kg/yr, what is the estimated gas flux from underneath the final landfill cover area?

The gas flux, Φ_g , can be estimated as follows:

$$\Phi_g = r_g \left(\frac{V_{waste}}{A_{cover}} \right) \varrho_{waste} \tag{1}$$

$$\Phi_g = \frac{0.00624 \text{ m}^3}{\text{kg yr}} \times \frac{1 \text{ yr}}{8,760 \text{ hr}} \times \frac{30 \text{ m}^3}{\text{m}^2} \times \frac{800 \text{ kg}}{\text{m}^3} = 0.017 \frac{\text{m}^3}{\text{hr m}^2}$$

END OF EXAMPLE 1

4 SLOPE STABILITY CALCULATIONS INCORPORATING GAS PRESSURES USING AN INFINITE-SLOPE ANALYSIS

A general cross section of an infinite landfill slope with a final cover is shown in Figure 1a. The free-body diagram and force polygon for a vertical slice of the cover section to the interface just below the geomembrane are shown in Figure 1b. Because of the hydraulic break provided by the barrier geosynthetic (assumed to be a geomembrane), seepage forces that may occur in the cover soils above the geomembrane have no influence on the stability of the lower geomembrane interface. Therefore, separate slope stability analyses are required for the upper and lower geomembrane interfaces. The stability analysis presented herein is only for the lower geomembrane interface, where gas pressures can potentially occur.

The effective normal stress, σ', at the base of the slice in Figure 1b is given by:

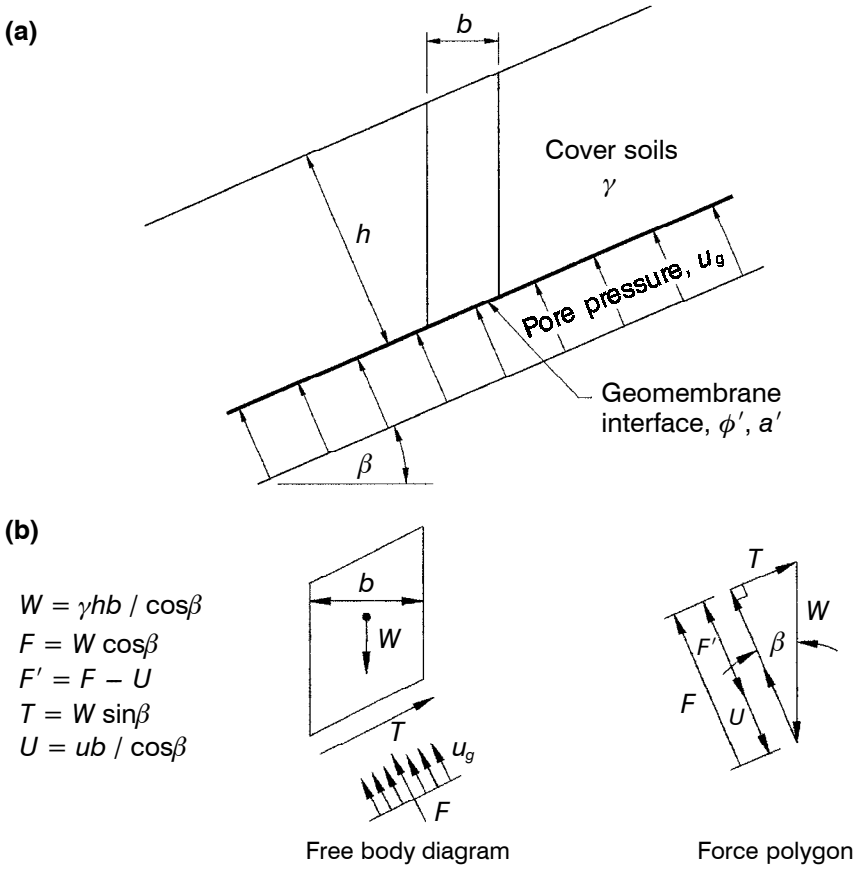

Figure 1. Infinite slope stability with pore pressures below geomembrane: (a) infinite slope geometry and material parameters; (b) forces on a representative slice of width, *b*.

$$\sigma' = \frac{F'}{b/\cos\beta} = h\,\gamma\,\cos\beta - u_g \tag{2}$$

where: F' = effective normal force; b = width of a representative slice; β = slope angle from the horizontal; h = thickness of cover soil normal to the slope; γ = average total unit weight of the soil; and u_g = gas pore pressure.

The tangential shear stress, τ, exerted on the slice is:

$$\tau = \frac{T}{b/\cos\beta} = h\,\gamma\,\sin\beta \tag{3}$$

where T is the tangential force.

The resisting shear strength, R, at the base of the slice is:

$$R = a' + \sigma' \tan\phi' \tag{4}$$

where: a' = effective geomembrane-soil interface adhesion parameter; and ϕ' = effective geomembrane-soil interface friction angle parameter.

The factor of safety is defined as the resisting shear strength divided by the driving shear stress:

$$FS = \frac{R}{\tau} = \frac{a' + (h\,\gamma\,\cos\beta - u_g)\,\tan\phi'}{h\,\gamma\,\sin\beta} \tag{5}$$

Presuming that the material properties and geometry are fixed for a specific design, the designer must then select a minimum allowable factor of safety, FS_{allow}, and calculate a maximum allowable gas pressure, $u_{(g\text{-}allow)}$. This can either be done iteratively using Equation 5, or solved explicitly:

$$u_{(g-allow)} = h\,\gamma\,\cos\beta - \frac{(FS_{allow}\,h\,\gamma\,\sin\beta - a')}{\tan\phi'} \tag{6}$$

Example 2. Cover Slope Stability Analysis to Determine Maximum Allowable Gas Pore Pressure

A final cover system on a 1V:3H slope (18.4°) consists of the following elements, from top to bottom:

- final cover soils above a drainage layer of thickness, h = 0.9 m, with an average unit weight, γ = 15.7 N/m^3; and
- geomembrane over a sand layer with ϕ' = 27° and a' = 0.

What is the variation in the factor of safety, *FS*, for gas pressures ranging from 0 to 4 kPa?

Equation 5 is used to calculate *FS* values, which are plotted against the variation in the assumed gas pressure as shown in Figure 2. The results show that even for a relatively strong interface between the geomembrane and underlying sand (ϕ' = 27°), very little excess gas pressure (approximately 0.3 kPa) can be tolerated before the factor of safety drops below 1.5. In selecting a value for $u_{(g\text{-}allow)}$, the designer needs to use judgment regarding an acceptable *FS* for this condition, noting that in most cases the gas flux diminishes over time. Also, the gas pressure is not uniform under the cover, as discussed in the Section 5.

END OF EXAMPLE 2

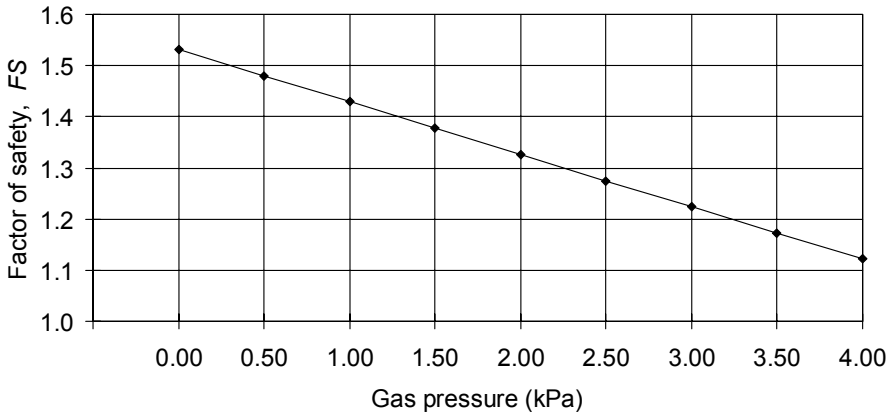

Figure 2. Solution for Example 2.

5 DESIGN OF GAS PRESSURE RELIEF SYSTEM

5.1 Proposed Gas Pressure Relief System Geometry

The vent system immediately below a landfill cover barrier system conceptually consists of a transmissive gas-relief layer with occasional outlets that penetrate the cover system. The gas-relief layer may only consist of the uppermost layer of waste itself, or it can be a permeable sand or geosynthetic layer. The gas-relief layer can be enhanced by the inclusion of intermittent, gravel-filled trenches or strip drains of greater permeability than the gas-relief layer to aid in the transmission of gas to the outlets. The outlets may be vents either going directly to the atmosphere, or connected to an active (vacuum) gas collection system. These surface gas-relief features are in addition to, and are a separate consideration from, any other gas collection systems such as vertical or horizontal gas wells that penetrate deeper into the waste.

For purposes of the model proposed in the current paper, the surface gas-relief layer is assumed to be composed of the following three primary elements:

- gas-relief layer;
- series of parallel trenches or strip drains (the term "strip drains" is used in the remainder of the paper), at a regular spacing, *D,* that collect gas from the gas-relief layer and are more permeable than the gas-relief layer to allow the gas to be conveyed to the outlets; and
- outlet points for the strip drains.

5.2 Derivation of Design Equations

Figure 3a shows a typical landfill slope cross section, with an emphasis on the gas collection layer below the barrier layer. In the cross section two benches are shown that

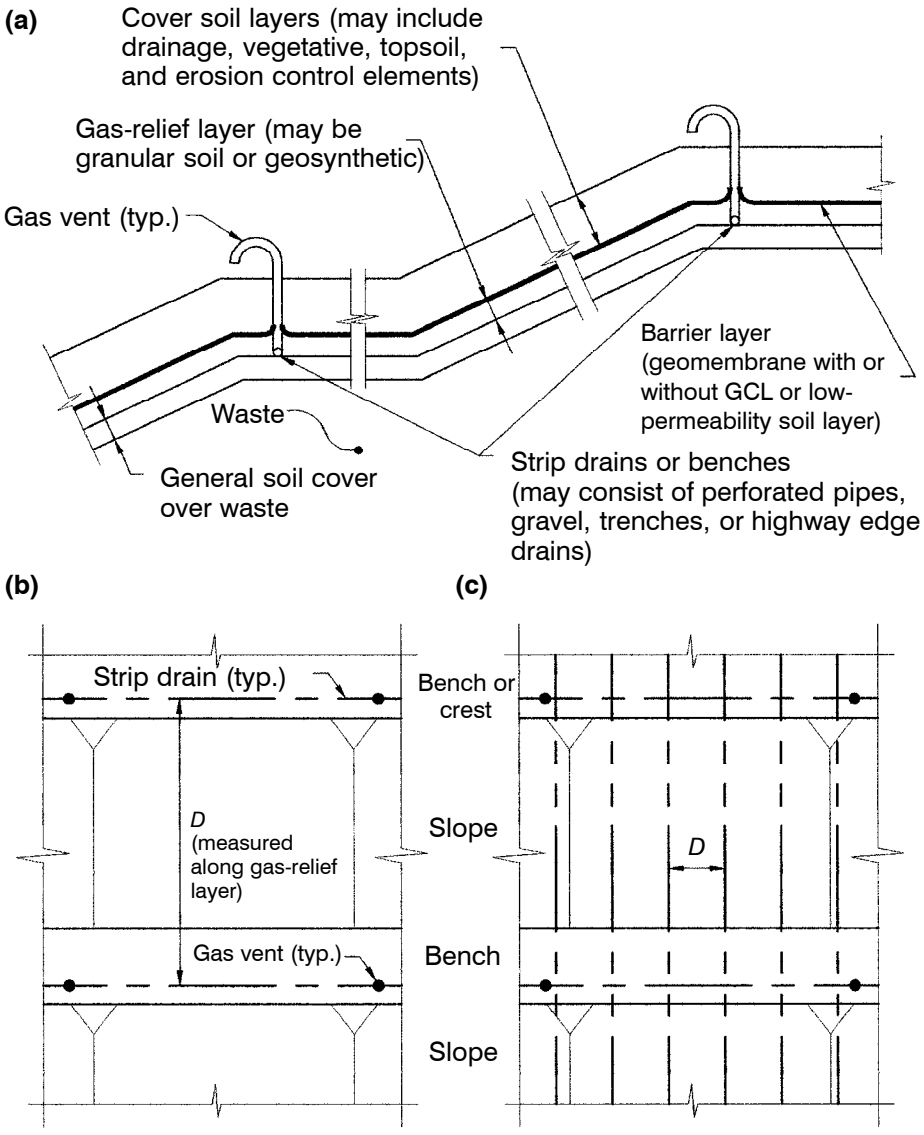

Figure 3. Schematic showing the design elements of the gas-relief layer: (a) profile of final cover with gas-relief layer and strip drains; (b) plan view of strip-drain layout on benches only; (c) plan view of strip-drain layout on slopes and benches.

can just as well be the crest and toe of the slope for small landfills. Strip drains, which can be perforated pipes, gravel-filled trenches, or geosynthetic highway edge drains, are shown running longitudinally along the benches. The distance *D* is defined as the slope distance between the strip drains. Figure 3b is a schematic plan view of the strip-

drain layout and also indicates that outlet points (in this case, vents to the atmosphere) can be intermittently located along the strip drains to relieve the collected gas.

In the event that the strip-drain spacing between benches is found to be inadequate, additional strip drains can be connected in the slope direction between benches. This is illustrated in Figure 3c where the spacing *D* is now defined as the distance between the drains running up and down the slope. In this case, the strip drains along the benches serve as headers.

One of the principles illustrated in the preceding discussion is that the orientation of the strip drains does not matter. In other words, because the unit weight of landfill gas is approximately equal to that of air, the gas travels upslope as easily as downslope (or laterally), and the elevation head does not influence the calculations.

The derivation of the relationship between the strip-drain spacing, *D*, incoming gas flux rate, gas transmissivity of the gas-relief layer, and pressure in the gas-relief layer is similar to the design of the drainage layer and drainage layer outlets, in the cover above the geomembrane, presented by Thiel and Stewart (1993). The derivation is based on Darcy's law, which applies to laminar fluid flow in porous media. (A proof of the applicability of laminar flow in this situation is discussed in Section 6.3.) The derivation steps are as follows:

1. Consider a unit-width surface area between strip drains as shown in Figure 4a. Figure 4b illustrates a cross section between two strip drains, showing the gas flux uniformly entering the gas-relief layer from the waste below. Ideally, the gas flow is symmet-

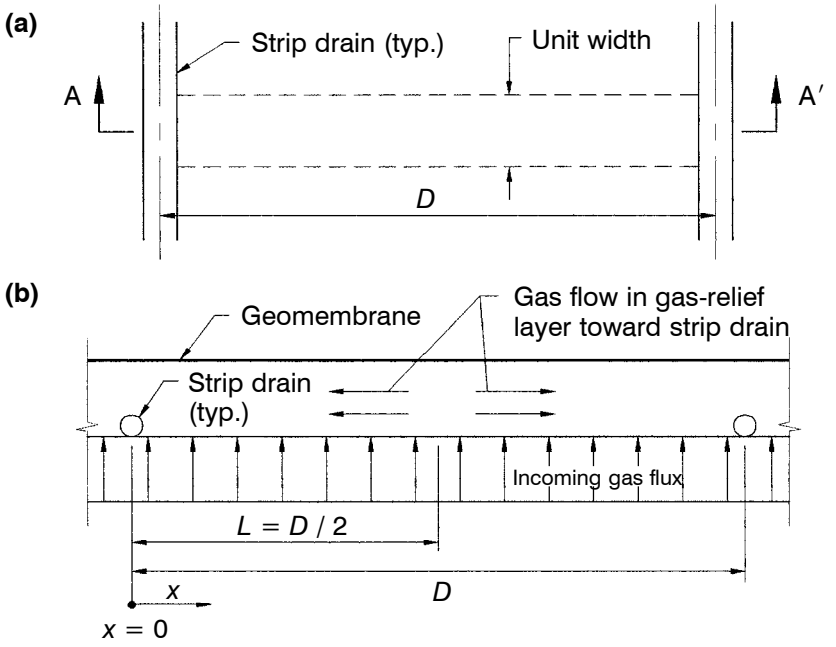

Figure 4. Model of gas flow to strip drains: (a) plan view; (b) cross-section A-A′.

ric about the centerline between the strip drains, thus, only the half-distance, L, where $L = D/2$, must be considered. Figure 4 identifies the variable distance x that begins at one of the strip drains and increases toward the centerline.

2. Figure 5 illustrates how the volume of gas being carried in the gas-relief layer varies linearly from zero at $x = L$, to a maximum value at $x = 0$. The volume of gas per unit width can be written in terms of the gas flux as:

$$Q_x = \Phi_g (L - x) \tag{7}$$

where Q_x is the volumetric flow rate of gas per unit width at any point x in the gas-relief layer.

3. The flow of gas in the gas-relief layer can be assumed to follow Darcy's law, which can be written in terms of the pressure gradient as follows:

$$Q_x = \left(\frac{k_g}{\gamma_g}\right) A \left(\frac{\mathrm{d}u_g}{\mathrm{d}x}\right) = \left(\frac{k_g}{\gamma_g}\right)(t \times 1)\left(\frac{\mathrm{d}u_g}{\mathrm{d}x}\right) = \left(\frac{k_g\, t}{\gamma_g}\right)\left(\frac{\mathrm{d}u_g}{\mathrm{d}x}\right) \tag{8}$$

where: k_g = coefficient of permeability to gas (or, gas permeability) for the gas-relief layer; γ_g = gas unit weight; A = cross-sectional flow area, which is the thickness of the layer, t, multiplied by a unit width; and $\mathrm{d}u_g/\mathrm{d}x$ = pressure gradient.

4. The transmissivity of the gas-relief layer, Ψ_g, can be defined as the gas permeability of the gas-relief layer multiplied by its thickness:

$$\Psi_g = k_g\, t \tag{9}$$

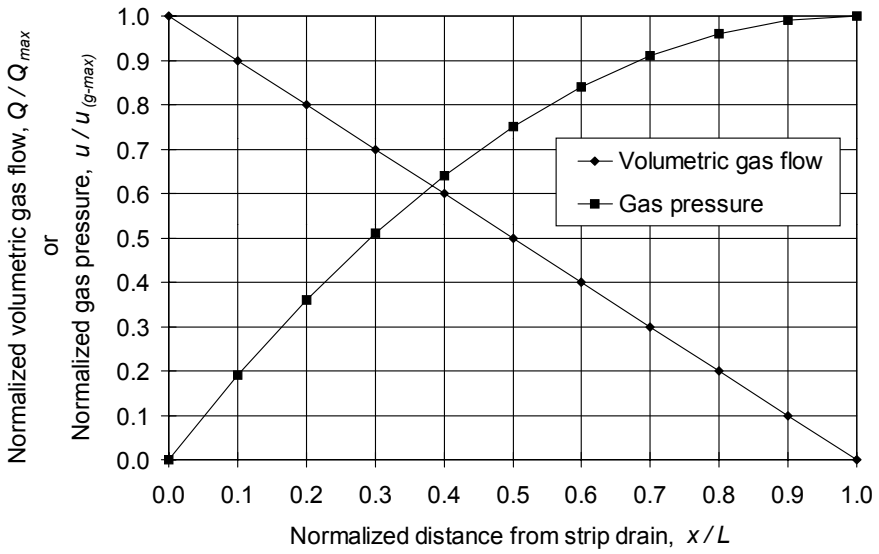

Figure 5. Normalized gas pressure and volume versus the distance from the strip drain.

Combining Equations 7, 8, and 9 gives:

$$\Phi_g (L - x) = \frac{\Psi_g}{\gamma_g} \frac{du_g}{dx} \tag{10}$$

5. Equation 10 can be rearranged to solve for u_g by integrating with respect to x:

$$u_g(x) = \frac{\Phi_g \gamma_g}{\Psi_g} \int_0^x (L - x)dx = \frac{\Phi_g \gamma_g}{\Psi_g} \left(Lx - \frac{x^2}{2} \right) \tag{11}$$

where $u_g(x)$ is the gas pressure at any distance x from a strip drain.

The normalized gas pressure is plotted in Figure 5 as a function of the distance from the strip drain. From Figure 5 and Equations 10 and 11, the following is observed:

- The pressure gradient, du_g/dx, varies linearly with distance x. The pressure gradient is a maximum at $x = 0$ (where the gas volume is greatest), and is zero at $x = L$ (where there is essentially no gas flow).
- The gas pore pressure varies as a polynomial function of distance. The pressure is zero at $x = 0$ (i.e. it is at the backpressure value in the strip drain). The maximum gas pore pressure at $x = L$ is:

$$u_{(g-max)} = \frac{\Phi_g \gamma_g}{\Psi_g} \left(\frac{L^2}{2} \right) \tag{12a}$$

or in terms of the strip-drain spacing, D:

$$u_{(g-max)} = \frac{\Phi_g \gamma_g}{\Psi_g} \left(\frac{D^2}{8} \right) \tag{12b}$$

Using Equation 12b, the distance D can be written in terms of the maximum pressure as follows:

$$D = \sqrt{\frac{8\, u_{(g-max)}\, \Psi_g}{\Phi_g \gamma_g}} \tag{13}$$

Although Equation 13 can be used conservatively to solve for the strip-drain spacing, it is reasonable that engineering judgment may be applied to select a gas pressure less than the maximum pressure for use in the stability analysis. For example, it is reasonable to assume that the gas pressure at $x = L/2$ is an appropriate choice for the design gas pressure, $u_{(g\text{-}allow)}$, because the slope stability calculation involves an area, rather than a point location. From Equation 11 (or Figure 4c) it can be determined that $u_{g\text{-}(L/2)} = 0.75(u_{(g\text{-}max)})$.

5.3 Backpressure Considerations

The calculation of the gas pressure gradient described in Section 5.2 is relative to the gas pressure in the strip drains. The pressure in the strip drains relative to the gas-relief layer is referred to as a backpressure because a certain amount of pressure is needed in the strip drains to cause the gas to flow from the strip drains to the vents, which are at atmospheric pressure (unless the system is under vacuum).

The backpressure required in the strip drains is a function of the strip-drain cross section, flow rate, and length. To establish a relative example, Figure 6 is provided to show the required backpressure in a 76 mm diameter smooth pipe as a function of the flow rate and length of pipe. Figure 6 shows, for example, that 187 Pa are required to cause 0.0274 m^3/s of gas to flow through 30 m of the selected pipe. Assuming a relatively permeable strip drain is provided, which is at least equivalent to a 76 mm diameter pipe, it seems reasonable that a backpressure of 250 Pa is conservative for most cases. If the strip-drain system is connected to an active vacuum system, the backpressure can be a negative value, which is beneficial to slope stability.

6 DISCUSSION OF GAS TRANSMISSIVITY COMPARED TO WATER TRANSMISSIVITY FOR SOILS AND GEOSYNTHETICS

6.1 Intrinsic Permeability

Use of Equations 12 or 13 requires the designer to select, or back-calculate, the gas-relief layer transmissivity value, Ψ_g . However, there is little, if any, testing or manufacturer data available regarding the gas transmissivity of soils or geosynthetics. Therefore, the designer usually resorts to assuming or specifying an equivalent hydraulic (water) transmissivity. In theory, the gas transmissivity can easily be calculated from the water transmissivity using the concept of intrinsic permeability.

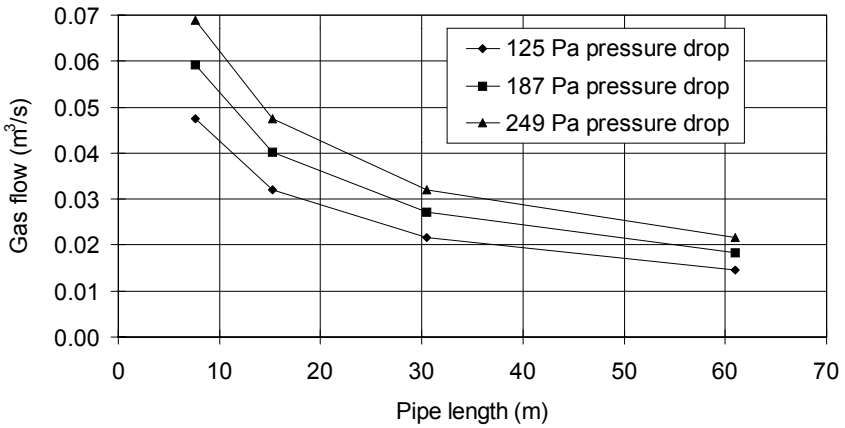

Figure 6. Flow capacity for a 76 mm diameter pipe versus length of pipe for various pressure drops.

Standard civil engineering practice that deals with the seepage of water through soils utilizes a constant, herein called k_w , to represent the proportionality between the flow rate of water, Q_w , and the area, A, times the dimensionless water gradient, i_w , between the two ends of flow. Darcy's law for water is written as:

$$Q_w = k_w \, i_w \, A \tag{14}$$

This result was deduced empirically through experimentation by H. Darcy in 1856 when he studied water flow through sand filters. The units for k_w are length per unit time. The value of k_w is characteristic of the soil tested and is valid for water at a specified temperature. In essence, the value of k is dependent on both the medium in question (e.g. a certain soil or geosynthetic) and the properties of the fluid.

Succeeding investigators sought to evaluate the range of validity of Equation 14 and determine the physical basis for its validity. One of the results of these investigations was the ability to define an intrinsic permeability characteristic of the medium in question that is entirely independent of the nature of the fluid. (See, for example, Lambe and Whitman (1969), pp. 287-289; McWhorter and Sunada (1977), pp. 65-71; or, for an excellent analytical and historical discussion, Muskat (1937)). The resulting reformulation of Darcy's law is:

$$Q_f = K \frac{\gamma_f}{\mu_f} \, i_f \, A \tag{15}$$

where: Q_f = volumetric flow rate of the fluid; γ_f = unit weight of the fluid; μ_f = dynamic viscosity of the fluid; i_f = fluid gradient; and K = intrinsic permeability of the medium (independent of the fluid) with units of length squared. Comparing Equations 14 and 15 allows the relationship between the standard civil engineering coefficient of permeability and the intrinsic permeability to be developed as follows:

$$k_f \, i_f \, A = K \frac{\gamma_f}{\mu_f} \, i_f \, A \tag{16a}$$

whereby the coefficient of permeability of a medium to any given fluid, k_f , can be solved knowing the intrinsic permeability of the medium, K, and the properties of the fluid as follows:

$$k_f = K \frac{\gamma_f}{\mu_f} \tag{16b}$$

Because K is a constant independent of the type of fluid, the ratio between the coefficients of permeability for two different fluids (denoted by subscripts 1 and 2) can be determined:

$$\frac{k_1}{k_2} = \frac{\mu_2}{\mu_1} \frac{\gamma_1}{\gamma_2} \tag{17}$$

Using Equation 17, the design of a gas-relief layer can now be accomplished by converting the required gas transmissivity to a required coefficient of permeability to water

(or, water permeability), k_w . All that is required are the physical properties of the fluids of concern (i.e. density and viscosity), which are easily obtained from published literature. (The important physical properties of water, air, carbon dioxide, methane, and landfill gas are presented in Table A-1 of the Appendix.) The validity of Equation 17 has been experimentally proven by Muskat (1937, p. 93, Table 7) for sand media that have k_w values ranging from 1×10^{-5} to 1×10^{-3} m/s. The experiments performed by Muskat showed that the intrinsic permeability of these same sands to air was identical to that measured for both water and carbon tetrachloride.

Example 3. Back-Calculation of Equivalent Water Permeability from Required Gas Permeability

Assume that, through iteration of Equation 13, a designer determines that the minimum required landfill gas transmissivity for a 0.3 m thick layer of sand is 0.0003 m^2/s. What is the equivalent water permeability, k_w ?

Rearranging Equation 9:

$$k_g = \frac{\Psi_g}{t} = \frac{0.0003}{0.3} = 0.001 \ \frac{\text{m}}{\text{s}}$$

From Equation 17 and Table A-1 in the Appendix:

$$k_w = k_g \frac{\mu_g}{\mu_w} \frac{\gamma_w}{\gamma_g} = 0.001 \ \frac{\text{m}}{\text{s}} \left(\frac{1.32 \times 10^{-5} \ \text{N–s/m}^2}{1.01 \times 10^{-3} \ \text{N–s/m}^2} \right) \left(\frac{9,797 \ \text{N/m}^3}{12.8 \ \text{N/m}^3} \right) = 0.01 \ \frac{\text{m}}{\text{s}}$$

END OF EXAMPLE 3

From Example 3, it can be noted that the water permeability of the soil is conveniently almost a factor of 10 larger than its landfill gas permeability. (Note that the calculations presented in the current paper assume that the gas is at standard temperature. Technically, the gas permeability should be adjusted for temperature due to viscosity changes. In landfills, the gas temperature is typically higher than 20°C; however, the change in viscosity with temperature for gases is much less than for water. It is also interesting to note that gases behave differently than water in that the viscosity increases as the temperature increases.)

The principle of intrinsic permeability is considered valid for granular soils and probably most geosynthetic drainage layers, but is not valid for silts and clays where the polarity of the fluid and electro-osmotic potentials begin to have a significant influence on the measured flow rates. In the case of finer-grained soils, the coefficients of permeability must be measured on a fluid-specific basis. However, finer-grained soils are generally not appropriate for a gas-relief layer in any case.

6.2 Gas Permeability for Partially Saturated Soils

If the gas-relief layer is a granular soil, it is reasonable to assume that the soil holds a certain amount of capillary water either due to rain during construction, or from condensate underneath the geomembrane. Note that condensate water is prevalent under landfill covers due to landfill gas, which is typically saturated. A sand in this application

would probably be at (or possibly slightly above) its saturation field capacity. Guidance on the saturation field capacity of typical sands can be found in the reference documents for the HELP computer program (Schroeder et al. 1994).

The reduction in gas permeability due to partial saturation of the sand layer can be estimated using the Brooks and Corey relationship as reported by Fredlund and Rahardjo (1993):

$$k_g = k_d (1 - S_e)^2 (1 - S_e^{(2+\lambda)/\lambda}) \tag{18}$$

$$S_e = \frac{S - S_r}{1 - S_r} \tag{19}$$

where: k_g = gas permeability under given moisture conditions; k_d = coefficient of permeability to air (or, air permeability) for a dry soil ($S = 0$); λ = pore-size distribution index (typical values range from 2 for porous rocks, to infinity for uniform sands); S_e = effective degree of saturation; and S_r = residual degree of saturation at which point an increase in matrix suction does not produce an appreciable change in the degree of saturation, S. Typical values for residual saturation are presented by Schroeder et al. (1994, p. 13, Figure 2).

Example 4. Air Permeability Calculation for a Moist Sand

Given the following parameters:

- sand with a saturated water permeability, $k_w = 6 \times 10^{-5}$ m/s (actual laboratory value);
- field moisture content of sand, $w = 16.9\%$ (actual laboratory value);
- dry unit weight of the sand, $\gamma_d = 13.61$ kN/m^3 (actual laboratory value);
- sand porosity, $n = 0.46$ (from Peck et al. (1974), for a loose, uniform sand that approximately matches the dry unit weight value used for this example);
- $S_r = 0.05$; and
- pore-size distribution index, $\lambda = 4$ (value for natural sand deposits reported by Fredlund and Rahardjo (1993)).

What is the air permeability of the moist sand?

The degree of saturation of the soil, S, is given by the following:

$$S = \frac{w}{n}\frac{\gamma_d}{\gamma_w} = \frac{0.169}{0.46}\left(\frac{13.61 \text{ kN/m}^3}{9.8 \text{ kN/m}^3}\right) = 0.51 \tag{20}$$

where: γ_w = unit weight of water; and n = soil porosity.

From Equation 19:

$$S_e = \frac{(0.51 - 0.05)}{(1 - 0.05)} = 0.484$$

Using Equation 17 and the appropriate values for unit weight and viscosity of water and air (see the Appendix), the value of the dry-air permeability of the sand can be calculated as follows:

$$k_d = (6 \times 10^{-5}\ \text{m/s}) \left(\frac{1.01 \times 10^{-3}\ \text{N–s/m}^2}{1.79 \times 10^{-5}\ \text{N–s/m}^2} \right) \left(\frac{11.8\ \text{N/m}^3}{9,800\ \text{N/m}^3} \right) = 4.06 \times 10^{-6}\ \text{m/s}$$

From Equation 18, the air (gas) permeability under moist conditions is:

$$k_g = (4.06 \times 10^{-6}\ \text{m/s})\ (1 - 0.484)^2\ (1 - 0.484^{1.5}) = 7.2 \times 10^{-7}\ \text{m/s}$$

END OF EXAMPLE 4

In Example 4, which is based on laboratory data from a field sample, the average laboratory measured gas permeability of the moist sand was 8×10^{-7} m/s, which is in good agreement with the theoretically derived value. Note that the ratio of k_g / k_d is approximately 0.18, i.e. the gas permeability of the sand was reduced by over 80% due to the presence of field moisture.

Using the typical values of moisture field capacity for sands presented by Schroeder et al. (1994) and using the same calculations as in Example 4, indicates that the gas permeability of a typical sand can be reduced by 25 to 50%. Example 4, which uses actual field data, shows a considerably greater reduction in gas permeability because the field moisture content was greater than the static-drained field capacity. This is probably due to rainy weather during construction and the constant presence of moisture due to saturated landfill gas. Coarser sands are less saturated and retain better gas permeability. Based on limited field experience (as discussed in Example 4 and the case histories in Section 7) and the limited data presented in the literature, the following preliminary recommendations are put forward until more data is available:

1. For fine sands containing less than 10 to 15% fines, the field-gas permeability can be taken as the dry-gas permeability reduced by a factor of 5 to 10 (one-half order of magnitude to one order of magnitude) to account for the presence of field moisture.
2. For clean medium and coarse sands, the field-gas permeability can be taken as the dry-gas permeability reduced by a factor of 2 (one-half the dry value) to account for the presence of field moisture.

6.3 Validity of Darcy's Law for Typical Gas Gradients Expected Under Landfill Covers

As stated in Section 5.2, Darcy's law is only valid when fluid flow is laminar. It can be shown that the character of fluid flow depends on the relationship between the fluid velocity, density, viscosity, and characteristic diameter of the flow path. This relationship is expressed as the Reynolds number, R_e, as follows:

$$R_e = \frac{\varrho v d}{\mu_f} \tag{21}$$

where: ϱ = fluid density; v = fluid velocity; and d = characteristic flow dimension. The units must all be consistent to produce a dimensionless value for R_e.

In classical fluid mechanics, considering the flow of fluids in pipes, the flow is considered laminar for R_e values less than 2,000, and the characteristic dimension, d, is the pipe diameter (Mott 1979). For R_e values greater than 4,000, the flow in pipes is generally considered turbulent. For R_e values between 2,000 and 4,000 it is very difficult to predict which type of flow exists.

In porous media such as sands, investigators have generally taken the characteristic diameter, d, as a representative grain size of the soil. Physically, it seems more appropriate to have the term d represent an average pore size rather than a grain diameter. However, direct measurement of pore sizes is very difficult, and most historic correlations of Reynolds numbers for flow through soils have referred to the averages of actual grain diameters obtained from sieve analyses (Muskat 1937.) The results of experiments involving flow rates of various fluids (liquids and gases) through soils indicate that the critical Reynolds number below which the flow is laminar is between 1 and 10, with most references conservatively identifying a value of 1 as a safe limit for the applicability of Darcy's law. In this case, the velocity term, v, is the macroscopic velocity obtained by dividing the flow rate by the entire cross-sectional area of the soil medium. (Note that this is not the actual velocity of the liquid in the pores.)

Given these parameters, it can now be verified that the flow of landfill gas in a porous medium below a landfill cover is usually expected to be laminar. Examples 5a, 5b, and 5c below confirm this assumption for sand, geonets, and nonwoven, needle-punched (NWNP) geotextile gas-relief layers, respectively, by showing that the Reynolds numbers for the assumed situations are less than the critical Reynolds numbers for laminar flow.

Example 5a. Reynolds Number for Gas Flow Through a Fine-to-Medium Sand

The following parameters are known:

- gas flux from Example 1, $\Phi_g = 0.017$ m^3/hr-m^2;
- spacing between strip drains of 30.5 m;
- 0.3 m thick sand gas-relief layer; and
- average sand particle size of 0.5 mm.

What is the Reynolds number, R_e, and is the flow laminar?

Using the flux rate from Example 1, the maximum gas flow rate, Q, from the half-distance between strip drains per unit width can be calculated as:

$$Q = \Phi_g \frac{D}{2}(\text{unit width}) = \left(0.017 \frac{\text{m}^3}{\text{hr m}^2}\right)\left(\frac{30.5 \text{ m}}{2}\right)(1 \text{ m})\left(\frac{\text{hr}}{3,600 \text{ s}}\right) = 7.2 \times 10^{-5} \frac{\text{m}^3}{\text{s}} \quad (22)$$

The flow velocity is calculated as:

$$v = \frac{Q}{A} = \frac{(7.2 \times 10^{-5} \text{ m}^3/\text{s})}{(0.3 \text{ m})(1 \text{ m})} = 2.4 \times 10^{-4} \frac{\text{m}}{\text{s}} \quad (23)$$

From Equation 21, the Reynolds number is calculated as:

$$R_e = \frac{\varrho v d}{\mu_f} = \frac{(1.31 \text{ kg/m}^3)\ (2.4 \times 10^{-4} \text{ m/s})\ (0.0005 \text{ m})}{(1.32 \times 10^{-5} \text{ kg/s–m})} = 0.012$$

The flow is laminar because $R_e << 1$.

END OF EXAMPLE 5a

Example 5b. Reynolds Number for Gas Flow Through a Geonet Composite

Given the same parameters as in Example 5a, except that a geonet composite replaces the sand layer, assume that the effective depth of the flow path through the geonet (accounting for encroachment from geotextiles) is 1.5 mm. What is the Reynolds number, *Re*, and is the flow laminar?

As in Example 5a, the velocity is calculated as:

$$v = \frac{Q}{A} = \frac{(7.2 \times 10^{-5} \text{ m}^3/\text{s})}{(0.0015 \text{ m})\ (1 \text{ m})} = 0.05 \ \frac{\text{m}}{\text{s}}$$

From Equation 21 the Reynolds number is calculated as:

$$R_e = \frac{\varrho v d}{\mu_f} = \frac{(1.31 \text{ kg/m}^3)\ (0.05 \text{ m/s})\ (0.0015 \text{ m})}{(1.32 \times 10^{-5} \text{ kg/s–m})} = 7.4$$

In this case, because the characteristic dimension of flow was the actual height of the flow path, and the calculated velocity is probably close to the true velocity of the fluid flow, the critical Reynolds number for laminar flow is probably close to that used for pipes, which is 2,000. This conclusion was also inferred by Williams et al. (1984). The flow is expected to be laminar because $7.4 << 2{,}000$.

END OF EXAMPLE 5b

Example 5c. Reynolds Number for Gas Flow Through a Nonwoven, Needle-Punched (NWNP) Geotextile.

Given the same parameters as in Example 5a, except that a polypropylene NWNP geotextile replaces the sand layer, assume that the geotextile fibers are 45 denier (very coarse) and an average geotextile thickness of 3 mm. Noting that the specific gravity of polypropylene is 0.91 and that the definition of denier is grams per 9,000 m of fiber, the average diameter of a fiber can be calculated as 8.36×10^{-5} m. Assume that the flow through the NWNP geotextile is analogous to flow through a soil when calculating the Reynolds number. That is, use the macroscopic average flow velocity, *Q/A*, and use the fiber diameter as the characteristic flow dimension. What is the Reynolds number, R_e, and is the flow laminar?

As in Example 5a, the velocity is calculated as:

$$v = \frac{Q}{A} = \frac{(7.2 \times 10^{-5}\ \text{m}^3/\text{s})}{(0.003\ \text{m})\ (1\ \text{m})} = 2.4 \times 10^{-2}\ \frac{\text{m}}{\text{s}}$$

From Equation 21 the Reynolds number is calculated as:

$$R_e = \frac{\varrho v d}{\mu_f} = \frac{(1.31\ \text{kg/m}^3)\ (2.4 \times 10^{-2}\ \text{m/s})\ (8.36 \times 10^{-5}\ \text{m})}{(1.32 \times 10^{-5}\ \text{kg/s–m})} = 0.20$$

Therefore, the flow is expected to be laminar because $R_e < 1$.

END OF EXAMPLE 5c

Examples 5a, 5b, and 5c employ typical gas flow parameters to be expected under a landfill final cover, and a reasonably wide spacing between strip drains. The results indicate that gas flow is generally expected to be laminar for all types of flow media. Note that the calculations in these examples are independent of the pressure gradients required to create the assumed flow rates. As discussed in Section 7, the pressure gradients required to pass the assumed gas flow may be unacceptably high for some of the flow media.

7 DESIGN CASE HISTORIES

7.1 Final Cover Design and Gas Collection for Coffin Butte Landfill, Corvallis, Oregon, USA

In 1996, 38,060 m^2 of a final cover was installed over a portion of Cell 1 at the Coffin Butte landfill. Most of the landfill cover rests on a 1V:3H slope. It is worthwhile noting that Cell 1 has been in place since 1977, filling stopped in 1992, and there is an active gas collection system working in part of the cell using vertical wells that were installed during cover construction.

The landfill cover cross section consists of the following elements, from bottom to top:

- foundation soil over waste;
- 150 mm thick sand gas-relief layer;
- 1.5 mm thick textured polyethylene geomembrane;
- 300 mm thick gravel drainage layer;
- geotextile filter; and
- 450 mm of topsoil and vegetation (grasses and legumes were planted).

The strip-drain spacing, D, is an average of 45 m. The gas-relief layer consists of a medium, poorly graded sand having an average grain size of 0.85 mm, and a coefficient of permeability, $k_w = 3 \times 10^{-4}$ m/s. The interface friction angle between the sand and the textured geomembrane was estimated to be 30°. The assumed unit weight of the cover materials is 16.5 kN/m^3.

After the cover was constructed, gas flows were monitored from the strip-drain header collection pipe. The gas was being extracted under a vacuum of approximately 124 Pa and was an average temperature of 25°C. The maximum flow rate observed was 0.045 m^3/s. Dividing the flow rate by the area yields a gas flux, $\Phi_g = 1.2 \times 10^{-6}\ m^3/s/m^2$. Note that this gas flow is only approximately 23% of what may have been estimated using Example 1. However, this amount of gas is impressive considering the age of the waste in the cell (i.e. most of the gas has already been generated and released), and the fact that much of the gas was being collected in an active collection system.

Given the relatively clean nature of the sand, the field gas permeability is assumed to be one-half the calculated dry gas permeability in accordance with the recommendations presented in Section 6.2. Using the results from Example 3 and Equation 17:

$$k_g = \frac{1}{2}(k_d) = \frac{1}{2}\left(\frac{k_w}{10}\right) = \frac{1}{2}\left(\frac{3 \times 10^{-4}\ \text{m/s}}{10}\right) = 1.5 \times 10^{-5}\ \text{m/s}$$

Given the thickness of the sand layer, the effective gas transmissivity, Ψ_g, can be calculated from Equation 9 as:

$$\Psi_g = k_g t = (1.5 \times 10^{-5}\ \text{m/s})(0.15\ \text{m}) = 2.25 \times 10^{-6}\ \text{m}^2/\text{s}$$

It is assumed that the measured vacuum on the strip-drain header offsets the backpressure in the strip drains, such that the backpressure in the gas-relief layer next to the strip drains is zero gage pressure. Using Equation 12b, the value of $u_{(g\text{-}max)}$ is calculated:

$$u_{(g-max)} = \left(\frac{D^2}{8}\right)\left(\frac{\Phi_g \gamma_g}{\Psi_g}\right) = \left[\frac{(45\ \text{m})^2}{8}\right]\left[\frac{(1.2 \times 10^{-6}\ \text{m}^3/\text{s/m}^2)\,(12.8\ \text{N/m}^3)}{(2.25 \times 10^{-6}\ \text{m}^2/\text{s})}\right] = 1,728\ \text{Pa}$$

Using Equation 5, the factor of safety, *FS*, is estimated:

$$FS = \frac{[\,(0.9\ \text{m})\,(16,500\ \text{N/m}^3)\,(\cos 18.4^\circ) - 1,728\ \text{N/m}^2]\,(\tan 30^\circ)}{(0.9\ \text{m})\,(16,500\ \text{N/m}^3)\,(\sin 18.4^\circ)} = 1.5$$

While *FS* = 1.5 appears to be a reassuring value for the completed project, note that during construction of the drainage layer on top of the geomembrane, the factor of safety dropped to less than 1.1 when the drainage layer was only 300 mm thick. One lesson to consider with regard to this case history is the effects of gas during construction. This lesson is highlighted in the following case history of a landfill cover that failed during construction.

7.2 Final Cover Sliding Failure, Confidential Project

A sliding failure occurred during the construction of a 6 ha final landfill cover project. The slope on which the failure occurred was inclined at 1V:4H and was 18 m high with no benches. The cover system design consisted of the following elements, from bottom to top:

- foundation soil over the waste;

- 300 mm thick gas-relief layer consisting of a fine sand with a measured water coefficient of permeability of 6×10^{-5} m/s;
- geosynthetic clay liner (GCL);
- polyvinyl chloride (PVC) geomembrane;
- 300 mm thick sand drainage layer;
- 300 mm thick vegetative soil layer; and
- 150 mm thick topsoil layer.

The design also included vertical gas vents at a 60 m spacing on a square grid. The gas vents consisted of 450 mm diameter borings 4.6 to 18.3 m deep, with a 150 mm diameter slotted PVC pipe. The area around the pipe was backfilled with pea gravel.

Failure occurred after the following elements had been constructed or placed:

- gas vents;
- sand gas-relief layer;
- GCL;
- geomembrane; and
- 3.2 ha had just been covered with a 300 to 600 mm thick layer of drainage sand.

The observed failure mode was the geomembrane stretching and then tearing at the top of the slope. The sand on top of the geomembrane, and the geomembrane, slid downslope along the geomembrane/GCL interface. The GCL did not appear to be distressed. However, a thin film of bentonite had extruded from the slit-film side of the GCL at the geomembrane interface.

As the failure progressed and rain eroded portions of the top sand drainage layer, large gas bubbles formed underneath the geomembrane. Even the exposed GCL appeared to be uplifted by gas pressures. Subsequent installation of 12 gas probes monitored over a two month period revealed an average gas pressure in the gas-relief layer of 1.7 kPa in the nine most critical locations. The probe measuring the highest pressures, an average of 3.3 kPa (average of 23 readings), had a single high reading of 4 kPa.

Shear strength testing was conducted on the PVC geomembrane/hydrated GCL interface over a normal load range of 2.4 to 12 kPa. The measured Mohr-Coulomb shear strength parameters were $\phi' = 16°$ and $a' = 0.5$ kPa. Using a moist sand unit weight of 17.3 kN/m^3 and a sand layer thickness of 300 mm, the factor of safety can be calculated from Equation 5 as follows:

$$FS = \frac{500\ \text{N/m}^2 + [(0.3\ \text{m})\ (17{,}300\ \text{N/m}^3)(\cos 14^\circ) - 1{,}700\ \text{N/m}^3]\ \tan 16^\circ}{(0.3\ \text{m})\ (17{,}300\ \text{N/m}^3)\ (\sin 14^\circ)} = 1.16$$

This factor of safety is still greater than one; however, the factor of safety is extremely sensitive to the shear strength parameters and the assumed pore pressure. A discussion of these sensitivities is provided by Liu et al. (1997). For example, by simply ignoring the very small y-intercept value, a', of the Mohr-Coulomb envelope, which is a very common practice and, in fact, is often recommended in the literature (Koerner and Soong 1998), the factor of safety reduces to 0.76. In addition, the following two other factors were suspected to drop the factor of safety to less than one:

- The gas pressure in many locations was greater than the overall average gas pressure. The gas pressure required to cause the factor of safety to drop below 1.0 was 2.5 kPa. The average gas pressure at two of the probes was above 2.5 kPa.
- The rapid increase in the unit weight of the cover sand during rain events caused an instantaneous pore water pressure increase at the interface between the geomembrane and the hydrated GCL. While the rain can saturate the sand in a matter of hours, it may take days for the excess water pressure to dissipate through the GCL. In fact, the slide movement was noted to greatly accelerate during rains and stabilize some time after the rains stopped. The increase in pressure due to the sand going from moist to saturated was on the order of 2.4 kPa. Added to the average gas pressure, this resulted in a factor of safety of approximately 1.0.

In this case history, no strip drains were provided in the gas-relief layer. In hindsight, this opportunity can be used to calculate the improvement in the factor of safety by installing strip drains. In this case, it was assumed that the effects of a rapid increase in unit weight of the cover due to rain increased the pore pressure by 2.4 kPa at the critical interface.

The equivalent landfill-gas permeability and transmissivity were calculated by first assuming a gas flux value as that estimated in Example 1, $\Phi_g = 5 \times 10^{-6}$ m^3/s/m^2. Then, the air permeability of the moist gas-relief layer was measured in the laboratory, k_{air} = as 8×10^{-7} m/s. Using Equations 17 and 9 to solve for the gas transmissivity:

$$k_g = k_{air} \frac{\mu_{air}}{\mu_{gas}} \frac{\gamma_{gas}}{\gamma_{air}}$$

$$= \left(8 \times 10^{-7} \ \frac{\text{m}}{\text{s}}\right)\left(\frac{1.79 \times 10^{-5} \ \text{N–s/m}^2}{1.32 \times 10^{-5} \ \text{N–s/m}^2}\right)\left(\frac{12.8 \ \text{N/m}^3}{11.8 \ \text{N/m}^3}\right)$$

$$= 1.2 \times 10^{-6} \ \frac{\text{m}}{\text{s}}$$

$$\Psi_g = k_g t = \left(1.2 \times 10^{-6} \ \frac{\text{m}}{\text{s}}\right)(0.3 \text{ m}) = 3.6 \times 10^{-7} \ \frac{\text{m}^2}{\text{s}}$$

Using Equations 5 and 12b, the variation in the factor of safety with a strip drain spacing, D, is graphically presented in Figure 7. Figure 7 shows a variation in FS from 1.4 with back-to-back strip drains (i.e. no gas pressure buildup), to $FS = 1.0$ with a strip drain spacing of 8.8 m. The close strip-drain spacing required for this case history was caused by the poor transmissivity of the sand. One of the lessons learned in this case is that fine sands, which may demonstrate relatively good water permeability, lose a large amount of their gas permeability due to the presence of field moisture (again, see Example 4, which was taken from this case history).

7.3 Laboratory Study of Gas Transmissivity of NWNP Geotextiles

When specifying a gas-relief layer, it is tempting to consider the use of a NWNP geotextile for three reasons. First, the thickness of the layer is small, which conceivably leaves more room for waste (compared to, say, a 300 mm thick layer of granular material). Second, the cost to supply and install a single geotextile may be less than either a

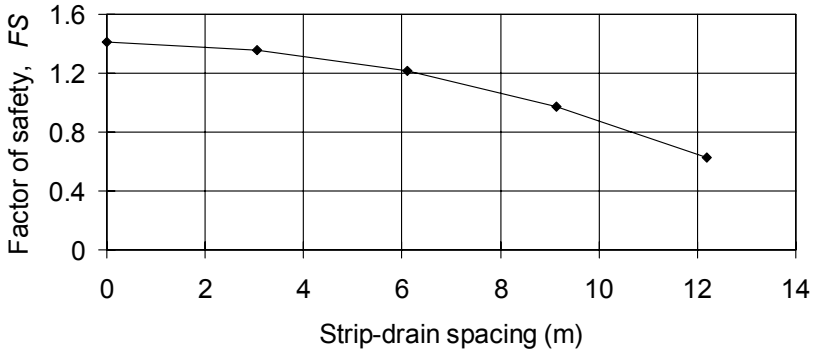

Figure 7. Solution for the sliding landfill cover failure case history.

geonet composite or a granular layer. Third, the construction time and efficiency is most desirable for a single geotextile compared to these other two alternatives.

There is limited test data available regarding the in-plane air transmissivity (or permeability) of geotextiles. Koerner et al. (1984) presents an interpretation of water and air transmissivity testing using a radial flow device. However, the data interpretation appears to have been flawed in that the authors did not take into account the gradient for the air testing, and the relationship between the water permeability and transmissivity test results does not appear to result in a realistic material thickness (the raw data is not provided in the paper). Therefore, the data reported by Koerner et al. (1984) cannot be used without further evaluation of the raw data.

Weggel and Gontar (1993) used the same radial flow device as Koerner et al. (1984) to study in-plane air flow through eight NWNP geotextiles. Weggel and Gontar provided a substantial amount of raw experimental data and a relatively thorough derivation of the flow analysis. Their testing appears to have been outside of the laminar flow region as indicated by the trends in the test data (i.e. permeability decreases with increasing gradient) and by calculation of the Reynolds number ($R_e > 1$ as per the calculation method used in Example 5c). Their empirically derived relationship results in, for example, a transmissivity value of approximately 1.5×10^{-7} m^2/s for a dry 3.7 mm thick geotextile (presumably 540 g/m^2) (this is approximately one-half the gas transmissivity of the fine sand described in the failure case history in Section 7.2).

Perhaps the most interesting data provided to the author of the current paper was from a manufacturer who had their products tested at an independent laboratory (Geocomp 1998), using a radial-flow device. Testing was performed on a suite of three NWNP polyester geotextiles, under both dry and wet conditions, at a normal load of 47.8 kPa. The relevant test data, and the author's interpretation of the data, are summarized in Table 1. No statement can be made concerning the accuracy of the results because the author was not involved in the testing and the test method is nonstandard. However, assuming a relatively high precision of the data, it is interesting to note the following:

Table 1. Radial air-flow test results for three NWNP polyester geotextiles (Geocomp 1998).

Data from laboratory report					Values calculated by author (1)			
Specimen	Pressure drop (kPa)	Specimen inner radius (m)	Specimen outer radius (m)	Air flow rate (m^3/s)	Assumed unit weight of air (N/m^3)	Calculated transmissivity for air (m^2/s)	Calculated (2) transmissivity for water (m^2/s)	Ratio wet to dry transmissivity (%)
6 dn/540 g/m^2 Dry	0.69	0.0635	0.1397	4.68×10^{-4}	11.8	1.00×10^{-6}	1.49×10^{-5}	
6 dn/540 g/m^2 Dry	1.38	0.0635	0.1397	9.16×10^{-4}	11.8	9.83×10^{-7}	1.46×10^{-5}	
6 dn/540 g/m^2 Dry	2.07	0.0635	0.1397	1.31×10^{-3}	11.8	9.36×10^{-7}	1.39×10^{-5}	
					Average	$\mathbf{9.74 \times 10^{-7}}$	$\mathbf{1.44 \times 10^{-5}}$	
6 dn/540 g/m^2 Wet	0.69	0.0635	0.1397	3.21×10^{-4}	11.8	6.89×10^{-7}	1.02×10^{-5}	
6 dn/540 g/m^2 Wet	1.38	0.0635	0.1397	6.00×10^{-4}	11.8	6.44×10^{-7}	9.53×10^{-6}	
6 dn/540 g/m^2 Wet	2.07	0.0635	0.1397	8.64×10^{-4}	11.8	6.18×10^{-7}	9.15×10^{-6}	
					Average	$\mathbf{6.50 \times 10^{-7}}$	$\mathbf{9.63 \times 10^{-6}}$	70%
15 dn/680 g/m^2 Dry	0.69	0.0635	0.1397	1.39×10^{-3}	11.8	2.98×10^{-6}	4.41×10^{-5}	
15 dn/680 g/m^2 Dry	1.38	0.0635	0.1397	2.56×10^{-3}	11.8	2.75×10^{-6}	4.07×10^{-5}	
15 dn/680 g/m^2 Dry	2.07	0.0635	0.1397	3.76×10^{-3}	11.8	2.69×10^{-6}	3.98×10^{-5}	
					Average	$\mathbf{2.81 \times 10^{-6}}$	$\mathbf{4.15 \times 10^{-5}}$	
15 dn/680 g/m^2 Wet	0.69	0.0635	0.1397	9.30×10^{-4}	11.8	2.00×10^{-6}	2.96×10^{-5}	
15 dn/680 g/m^2 Wet	1.38	0.0635	0.1397	1.71×10^{-3}	11.8	1.84×10^{-6}	2.72×10^{-5}	
15 dn/680 g/m^2 Wet	2.07	0.0635	0.1397	2.49×10^{-3}	11.8	1.78×10^{-6}	2.64×10^{-5}	
					Average	$\mathbf{1.87 \times 10^{-6}}$	$\mathbf{2.77 \times 10^{-5}}$	67%
45 dn/1,080 g/m^2 Dry	0.69	0.0635	0.1397	4.52×10^{-3}	11.8	9.69×10^{-6}	1.43×10^{-4}	
45 dn/1,080 g/m^2 Wet	0.69	0.0635	0.1397	3.37×10^{-3}	11.8	7.24×10^{-6}	1.07×10^{-4}	75%

Notes: dn = denier is a unit of measurement of the linear density of fibers, and is defined as the weight in grams per 9,000 m of fiber. Knowing the specific gravity of the geotextile polymer, an approximate average fiber diameter can be calculated. For example, assuming that the specific gravity of polyester is 1.3, the average fiber diameters of 6, 15, and 45 denier fibers are estimated to be 2.56×10^{-5}, 4.04×10^{-5}, and 7.00×10^{-5} m, respectively. (1) Data interpretation after method presented by Weggel and Gontar (1993). (2) Water transmissivity calculated from air transmissivity per Equation 17.

- The wet specimens lost 25 to 33% of their transmissivity, compared to the dry specimens.
- Going from a material with a linear density of 6 denier (dn) and a mass per unit area of 540 g/m^2, to 45 dn and 1,080 g/m^2, respectively, resulted in an order-of-magnitude increase in transmissivity. Such a large increase in transmissivity cannot be attributed simply to the doubling of the mass per unit area of the geotextile. Apparently, the larger fiber size (45 dn versus 6 dn) had a significant influence on the in-plane flow rate. The relative intensity of needle-punching for each specimen may also have an influence, but a description of these characteristics were not available to the author. These observations point to the need for a more complete description of NWNP geotextiles than is often reported in the literature or by testing laboratories.
- If the results are assumed to be approximately accurate, then it is interesting to note that the estimated in-plane water transmissivity of the 45 dn material has the equivalent water transmissivity of a 300 mm thick layer of sand having a coefficient of permeability of 4.7×10^{-4} m/s. This is approximately equivalent to the sand layer described for the Coffin Butte case history in Section 7.1. Because the effects of wetting the 45 dn geotextile appear to be less than the assumed wetting effects on sand in terms of effecting gas transmissivity, the 45 dn geotextile may have been an appropriate design substitute for the sand as the gas-relief layer in the Coffin Butte landfill.

It is interesting to compare the air transmissivity data described above to water transmissivity test results made available by a different manufacturer of a nominal 540 g/m^2 polyester geotextile (Hoechst Celanese Corp. 1991, test results for Trevira® 1155). The interpolated water transmissivity of this geotextile under a 47.8 kPa normal load is 1.55×10^{-5} m^2/s. This compares very well with the water transmissivity value of 1.44×10^{-5} m^2/s estimated for the equivalent Geocomp 6 dn, 540 g/m^2 polyester geotextile described above. This comparison either points to the validity of the concept of intrinsic permeability and relatively good accuracy of the testing performed, or is a coincidence of errors. Only additional, well-documented testing is able to answer which is true.

8 RECOMMENDATIONS AND DISCUSSION

The theoretical solution for gas flow presented in the current paper is undoubtedly more developed than the profession's ability to provide the basic input parameters to the model. To that extent, it may be found that the theoretical assumptions presented herein are incorrect when a more accurate understanding of landfill gas generation, flux, and flow mechanisms is attained. However, in lack of any other available procedures, the model presented in the current paper is meant to serve as a starting point, and has been qualitatively calibrated by two field experiences - one successful landfill cover design with gas flow measurements and one landfill cover failure attributed, in part, to excess gas pressures.

The key input parameter that requires more development is the assumed gas flux, which may cause pressures below a landfill cover to develop. To that end, additional

gas flow measurements below installed covers, such as that described for the Coffin Butte landfill, are useful. Gas pressure measurements, as described for the failure history, are also very useful.

The geosynthetics industry is also in need of good, well-documented test data for in-plane gas (typically air) transmissivity. The testing should be performed at relatively low pressure gradients representative of landfill gas collection requirements, where the flow is laminar as discussed in Example 5c. (However, higher-gradient tests with nonlaminar flow are conservative in that they result in lower transmissivity values.) The testing should be performed not only for dry geotextiles, but also on wet geotextiles at a simulated field moisture capacity obtained from soaking the geotextile and then letting it drain. When possible, it is useful to provide side-by-side testing of air and water transmissivity in the laminar flow region to verify that the concept of intrinsic permeability can be applied to geotextiles. The geotextiles being tested should be fully described in terms of their mass per unit area, fiber size, initial thickness, and polymer type.

The model presented herein is probably conservative because many successful landfill covers have been constructed without explicit considerations for gas pressures. However, the author has witnessed several cover construction projects that, even though successful in producing the end product, experienced significant landfill gas problems during construction. Whether the design procedures presented in the current paper or a different method are used, the author believes that all parties involved in the construction of the landfill final cover will be well served if highly permeable strip drains and a gas-relief layer are constructed below the cover system.

9 CONCLUSIONS

Slope stability of landfill cover systems incorporating geomembrane barriers can be compromised by pore pressures caused by landfill gas. This has been demonstrated by field failures in which gas pressures appeared to play a significant role.

Standard geotechnical and fluid mechanics engineering principles can be used to design final cover systems to accommodate potential landfill gas pressures. However, as is typical with many geotechnical problems, an estimation of the field gas pressures and volumes and other basic field parameters is not an exact science, and involves educated assumptions and experience.

Calculations and experimental evidence from the literature suggest that landfill gas flow rates in gas-relief layers are generally expected to be laminar, thus, Darcy's law applies. The fluid mechanics principle of intrinsic permeability can allow estimations of gas transmissivity and permeability to be made based on more well-known, or more easily obtained, values for water.

The analytical and design approach proposed herein to account for landfill gas pressures below covers appears to have been corroborated by one successful case history, and could have potentially predicted the failure of another case history. While the case histories described were not controlled and monitored to an extent that can be said to validate the proposed approach, the case history observations and measurements that were made do not contradict the proposed approach.

Limited laboratory test data suggests that coarse, heavy (e.g. 45 dn and 1,080 g/m^2) NWNP geotextiles may have adequate gas transmissivity under field conditions for

many typical situations. However, industry testing and design experience in this regard is sparse.

ACKNOWLEDGMENTS

The author is grateful to Mr. R. Marsh of Geocomp, Inc. for providing air transmissivity testing data for geotextiles, and to Mr. J. Pacey of Emcon Associates for his thoughtful review.

REFERENCES

Fredlund, D.G. and Rahardjo, H., 1993, "*Soil Mechanics For Unsaturated Soils*", John Wiley & Sons, Inc., New York, New York, USA, 517 p.

Geocomp, Inc., 1998, Personal communication with Ron Marsh, 1996-1998.

Hoechst Celanese Corp., 1991, Letter to author containing Trevira® Spunbond literature, including Tech Note 009-87.

Kavazanjian, E., 1998, "Current Issues in Seismic Design of Geosynthetic Cover Systems", *Proceedings of the Sixth International Conference on Geosynthetics*, IFAI, Vol. 1, April 1998, Atlanta, Georgia, USA, pp. 219-226.

Koerner, R.M., Bove, J.A. and Martin, J.P., 1984, "Water and Air Transmissivity of Geotextiles", *Geotextiles and Geomembranes*, Vol. 1, No. 1, pp. 57-73.

Koerner, R.M. and Soong, T.Y., 1998, "Analysis and Design of Veneer Cover Soils", *Proceedings of the Sixth International Conference on Geosynthetics*, IFAI, Vol. 1, Atlanta, Georgia, USA, April 1998, pp. 1-26.

Lambe, T.W. and Whitman, R.V., 1969, "*Soil Mechanics*", John Wiley & Sons, New York, New York, USA, 553 p.

Liu, C.N., Gilbert, R.B., Thiel, R.S. and Wright, S.G., 1997, "What Is An Appropriate Factor of Safety for Landfill Cover Slopes?", *Proceedings of Geosynthetics '97*, IFAI, Vol. 1, Long Beach, California, USA, March 1997, pp. 481-496.

McWhorter, D. and Sunada, D., 1977, "*Ground Water Hydrology and Hydraulics*", Water Resources Publications, Highlands Ranch, Colorado, USA, 290 p.

Mott, R.L., 1979, "*Applied Fluid Mechanics*", Second Edition, Charles E. Merrill Publishing Co., Columbus, Ohio, USA, 405 p.

Muskat, M., 1937, "*The Flow of Homogeneous Fluids Through Porous Media*", McGraw Hill, New York, New York, USA, 763 p.

Pacey, J.G., 1997, "Insights to Enhanced Landfill Gas Generation", *Proceedings of the Sixth International Landfill Symposium*, CISA, Vol. 1, Sardinia, Italy, pp. 359-368.

Peck, R.B., Hanson, W.L. and Thornburn, T.H., 1974, "*Foundation Engineering*", Second Edition, John Wiley & Sons, Inc., New York, New York, USA, 514 p.

Schroeder, P.R., Dozier, T.S., Zappi, P.A., McEnroe, B.M., Sjostrom, J.W. and Peyton, R.L., 1994, "*The Hydrologic Evaluation of Landfill Performance (HELP) Model - Engineering Documentation for Version 3*", USEPA, Cincinnati, Ohio, USA, 116 p.

Thiel, R.S. and Stewart, M.G., 1993, "Geosynthetic Landfill Cover Design Methodology and Construction Experience in the Pacific Northwest", *Proceedings of Geosynthetics '93*, IFAI, Vol. 3, Vancouver, British Columbia, Canada, March 1993, pp. 1131-1144.

Weggel, R. and Gontar, W.A., 1993, "In-Plane Air Flow Through Needle-Punched Nonwoven Geotextiles Under Normal Loading", *Geotechnical Testing Journal*, Vol. 16, No.2, pp. 207-215.

Williams, N., Giroud, J.P. and Bonaparte, R., 1984, "Properties of Plastic Nets for Liquid and Gas Drainage Associated with Geomembranes", *Proceedings of the International Conference on Geomembranes*, Denver, Colorado, USA, pp. 399-404.

NOTATIONS

Basic SI units are given in parentheses.

a'	=	effective geomembrane-soil interface adhesion parameter (Pa)
A	=	cross-sectional area of fluid flow (m^2)
A_{cover}	=	unit area of landfill cover (m^2)
b	=	width of representative slice in Figure 1 (m)
d	=	characteristic diameter or dimension for computing Reynolds number (m)
D	=	spacing between strip drains (m)
F	=	total normal force (N)
F'	=	effective normal force (N)
FS	=	factor of safety (dimensionless)
FS_{allow}	=	minimum allowable factor of safety (dimensionless)
h	=	thickness of cover soils normal to slope (m)
i_f	=	fluid gradient (dimensionless)
i_w	=	water gradient (dimensionless)
k_{air}	=	coefficient of permeability to air for soil or geosynthetic (m/s)
k_d	=	coefficient of permeability to dry air for soil or geosynthetic (m/s)
k_f	=	coefficient of permeability to particular fluid for soil or geosynthetic (m/s)
k_g	=	coefficient of permeability to gas for soil or geosynthetic (m/s)
k_w	=	coefficient of permeability to water for soil or geosynthetic (m/s)
k_1 , k_2	=	coefficient of permeability to Fluids 1 and 2, respectively for soil or geosynthetic (m/s)
K	=	intrinsic permeability (m^2)
L	=	half-spacing between strip drains (m)
n	=	soil porosity (dimensionless)

Q = volumetric flow rate (m^3/s)
Q_f = volumetric flow rate of fluid (m^3/s)
Q_{max} = maximum volumetric flow rate (m^3/s)
Q_w = volumetric flow rate of water (m^3/s)
Q_x = volumetric flow rate at specific location x (m^3/s)
R = resisting shear strength (Pa)
R_e = Reynolds number (dimensionless)
r_g = landfill gas generation rate (m^3/ kg-yr)
S = degree of saturation (dimensionless)
S_e = effective degree of saturation (dimensionless)
S_r = residual degree of saturation (dimensionless)
t = gas vent layer thickness (m)
T = tangential force to slope exerted by W (N)
u_g = gas pore pressure acting on bottom of geomembrane (Pa)
$u_{(g\text{-}allow)}$ = maximum allowable gas pore pressure (Pa)
$u_{g(L/2)}$ = gas pore pressure at $x = L/2$ (Pa)
$u_{(g\text{-}max)}$ = maximum gas pore pressure (Pa)
U = uplift force (N)
V_{waste} = unit volume of landfill waste (m^3)
v = fluid velocity (m/s)
w = soil moisture content (dimensionless)
W = total weight (N)
x = horizontal distance (m)
β = slope angle from horizontal (°)
γ = average total unit weight of fluid or soil (N/m^3)
γ_{air} = dry unit weight of air (N/m^3)
γ_d = dry unit weight of soil (N/m^3)
γ_f = unit weight of fluid (N/m^3)
γ_g = unit weight of gas (N/m^3)
γ_w = unit weight of water (N/m^3)
γ_1 , γ_2 = unit weight of Fluids 1 and 2, respectively (N/m^3)
λ = pore size distribution index (dimensionless)
μ_{air} = dynamic (absolute) viscosity of air ($N\text{-}s/m^2$)
μ_f = dynamic (absolute) viscosity of fluid ($N\text{-}s/m^2$)
μ_g = dynamic (absolute) viscosity of gas ($N\text{-}s/m^2$)
μ_w = dynamic (absolute) viscosity of water ($N\text{-}s/m^2$)
μ_1 , μ_2 = dynamic (absolute) viscosity of Fluids 1 and 2, respectively ($N\text{-}s/m^2$)
ν = kinematic viscosity (m^2/s)

ϱ = fluid density (kg/m^3)
ϱ_{waste} = landfill waste density (kg/m^3)
σ' = effective normal stress (Pa)
ϕ' = effective geomembrane-soil interface friction parameter (°)
Φ_g = gas flux from landfill surface (m^3/s/m^2)
Ψ_g = gas transmissivity of soil or geosynthetic (m^3/s/m)

APPENDIX

Table A-1. Fluid densities and viscosities.

Fluid	Density ϱ (kg/m^3)	Unit weight γ (N/m^3)	Dynamic viscosity μ (N-s/m^2 or kg/(s-m))	Kinematic viscosity $\nu = \mu/\varrho$ (m^2/s)
Water	9.99×10^2	9.80×10^3	1.01×10^{-3}	1.01×10^{-6}
Air	1.20×10^0	1.18×10^1	1.79×10^{-5}	1.48×10^{-5}
Carbon dioxide, CO_2	1.83×10^0	1.79×10^1	1.50×10^{-5}	8.21×10^{-6}
Methane, CH_4	6.66×10^{-1}	6.54×10^0	1.10×10^{-5}	1.65×10^{-5}
LFG: 55% CO_2 45% CH_4	1.31×10^0	1.28×10^1	1.32×10^{-5}	1.01×10^{-5}

Notes: Values for landfill gas (LFG) were assumed to be prorated as having the properties of 55% carbon dioxide and 45% methane. This ratio was used to match the LFG characteristics for the Coffin Butte case history, which may be different than other landfills. Values are at standard temperature and pressure.